Proceedings of the 3rd
RSI International Conference on Robotics and Mechatronics
October 7-9, 2015, Tehran, Iran

Eye-RHAS Manipulator: From Kinematics to Trajectory Control

Ebrahim Abedloo, Soheil Gholami, and Hamid D. Taghirad, *Senior Member, IEEE.*
Advanced Robotics and Automated Systems (ARAS), Industrial Control Center of Excellence (ICCE),
Faculty of Electrical Engineering, K.N. Toosi University of Technology, Tehran, Iran.
Email: {eabedloo, sgholami}@ee.kntu.ac.ir, taghirad@kntu.ac.ir.

***Abstract*—One of the challenging issues in the robotic technology is to use robotics arm for surgeries, especially in eye operations. Among the recently developed mechanisms for this purpose, there exists a robot, called Eye-RHAS, that presents sustainable precision in vitreo-retinal eye surgeries. In this work the closed-form dynamical model of this robot has been derived by Gibbs-Appell method. Furthermore, this formulation is verified through SimMechanics Toolbox of MATLAB . Finally, the robot is simulated in a real time trajectory control in a teleoperation scheme. The tracking errors show the effectiveness and applicability of the dynamic formulation to be used in the teleoperation schemes.**

Keywords*— *Eye Surgery, Eye-RHAS, Gibbs-Appell, Phantom Omni, Real Time Trajectory Control, SimMechanics.

I. Introduction

At present 285 million people are estimated to be visually impaired around the world: 39 million are blind and 246 million have low vision. For many eye diseases, surgery is the only possible treatment to improve vision or to stop further decrease in the visual quality and blindness [1]. Due to the dimensions and sensitivity, the most challenging issue in an eye surgery operation is the required accuracy. Vitreo-retinal surgery, which involves tissue manipulations in the posterior segment of the human eyeball, is one of the most precise operations accomplished by the surgeons, with a required accuracy smaller than hundred microns [2]. The natural tremors and physical constraints available in human's hand, besides some other problems, makes this type of eye surgery very challenging, which may be overcomed by proper use of a robotics arm.

Robotic eye surgery allows the surgeons to perform many kinds of complicated procedures with more precision and flexibility than that with conventional techniques. In general, robotic surgery is associated with minimally invasive surgery, i.e. the procedures performed through tiny incisions [3]. Besides other special privileges, this kind of surgery reduces the patient recovery time and pain. Among the recently developed systems for this means, there exists a robotic system that is dedicated to vitreo-retinal surgery. This robot, called Eye-RHAS, has been designed by Eindhoven University of Technology (TU/e). EyeRhas, shown in Fig. 1, uses two parallelograms to present a remote center of motion in eye surgeries. This robot has four degrees of freedom (DoF), including two prismatic and two revolute ones. The main advantages of this system compared with the other robots are the combination of both a dedicated master and slave robot, the integrated solution for mounting the system to the operating table, compactness, ease of installation and integrated electronics, and existance of an automated instrument changing system [2].

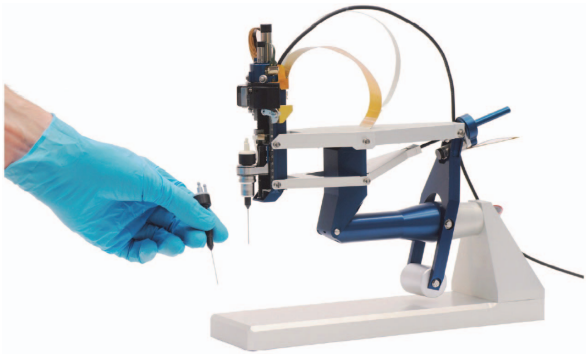

Fig. 1: Eye-RHAS manipulator [4].

In this work, a detailed mathematical analysis of this robot, including kinematics and dynamics, has been presented. To analyze the dynamical behavior of the mechanical systems, there are several methods such as: Lagrange, Newton-Euler, Gibbs-Appell (GA), and Kane formulations. Among them, GA method provides a simpler procedure to obtain the closed form dynamic models with respect to the well-know Lagrange or Newton-Euler methods. GA method was first introduced by Gibbs (1879) and then by Appell (1899) independently [5]. To see some further informations about these methods, one may review [6] and [7].

The obtained model has been verified by SimMechanics Toolbox of MATLAB [8]. Furthermore, due to the potential application of Eye-RHAS, a uni-lateral teleoperation system consists of a haptic device, namely, a PHANToM Omni [9] and a virtual Eye-RHAS model has been considered for teleoperation implementation. One may refer to [10] and [11] to have more insight about teleoperation systems. To evaluate this structure, an inverse dynamic control (IDC) scheme has been proposed and implemented on the system. Experimental results demonstrate the precision and applicability of the derived dynamics formulation.

978-1-4673-7234-3/15/$31.00 ©2015 IEEE

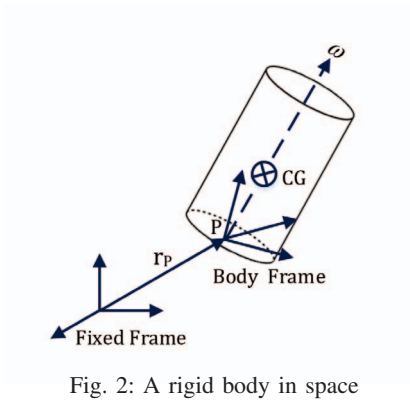

Fig. 2: A rigid body in space

II. Preliminaries

A. Manipulator Dynamics

By neglecting the effect of frictions and other possible disturbances, it is common [12] to write the closed-form dynamics model of a n-link rigid body manipulator in the form of:

$$\boldsymbol{H}(\boldsymbol{x})\ddot{\boldsymbol{x}} + \boldsymbol{C}(\boldsymbol{x},\dot{\boldsymbol{x}})\dot{\boldsymbol{x}} + \boldsymbol{G}(\boldsymbol{x}) = \boldsymbol{J}^{-T}\boldsymbol{U}, \tag{1}$$

in which, $\boldsymbol{H}(\boldsymbol{x})$ is the $n\times n$ symmetric positive definite matrix called manipulator inertia matrix, $\boldsymbol{x}$ is the $n \times 1$ array of relative generalized coordinates, $\boldsymbol{C}(\boldsymbol{x},\dot{\boldsymbol{x}})\dot{\boldsymbol{x}}$ is the $n \times 1$ array of centrifugal and Coriolis terms, $\boldsymbol{G}(\boldsymbol{x})$ is the $n \times 1$ array of gravitational effects on the manipulator, and $\boldsymbol{U}$ is the $n \times 1$ array of applied control inputs.

Equation (1) satifies two useful properties: 1) given a proper definition of $\boldsymbol{C}$, the matrix $\dot{\boldsymbol{H}} - 2\boldsymbol{C}$ is skew-symmetric, which means $\boldsymbol{H}$ and $\boldsymbol{C}$ are dependent; and 2) dynamics structure is linear in terms of a suitably selected set of robot and load parameters [13].

B. GA Dynamics Formulation

The GA or the acceleration energy function, plays a fundamental role in the GA dynamic formulation. This function is defined as [14]

$$S := \frac{1}{2}\int (\vec{\boldsymbol{a}}\cdot\vec{\boldsymbol{a}})\, dm, \tag{2}$$

where, dm is a element of the body and $\vec{a}$ denotes its acceleration. Consider a rigid body with a moving frame attached on it, called body frame. According to [14], the GA function of this body, shown in Fig. 2, can be written as

$$\begin{aligned} S = \frac{1}{2}\left[m\,(\vec{\boldsymbol{a}}_P\cdot\vec{\boldsymbol{a}}_P) + \vec{\boldsymbol{\alpha}}\cdot\frac{\partial\vec{\boldsymbol{h}}_P}{\partial t}\right] + \vec{\boldsymbol{\alpha}}\cdot\left[\vec{\boldsymbol{\omega}}\times\vec{\boldsymbol{h}}_P\right] \\ + m\,\vec{\boldsymbol{a}}_P\cdot[\vec{\boldsymbol{\alpha}}\times\vec{\boldsymbol{\rho}}] + m\,\vec{\boldsymbol{a}}_P\cdot[\vec{\boldsymbol{\omega}}\times(\vec{\boldsymbol{\omega}}\times\vec{\boldsymbol{\rho}})] + \Gamma(\vec{\boldsymbol{v}},\vec{\boldsymbol{\omega}}), \end{aligned} \tag{3}$$

where, the angular momentum, $\vec{\boldsymbol{h}}_P$ is defined as

$$\vec{\boldsymbol{h}}_P = \boldsymbol{I}_P\,\vec{\boldsymbol{\omega}}, \tag{4}$$

in which, $\boldsymbol{I}_P$ is a symmetric inertia tensor, and its time derivative in the body coordinate is zero, thus

$$\frac{\partial\vec{\boldsymbol{h}}_P}{\partial t} = \boldsymbol{I}_P\,\frac{\partial\vec{\boldsymbol{\omega}}}{\partial t} = \boldsymbol{I}_P\,\vec{\boldsymbol{\alpha}}. \tag{5}$$

Extending this concept for a multi-body system with n-DoF, GA function can be written as

$$S = S(\boldsymbol{x}_i, \dot{\boldsymbol{x}}_i, \ddot{\boldsymbol{x}}_i). \tag{6}$$

where, $\boldsymbol{x}_i,\ \dot{\boldsymbol{x}}_i$ and $\ddot{\boldsymbol{x}}_i$ are the generalized coordinates, and $i = \{1,\ 2,\ \ldots,\ n\}$. By partial differentiation of the GA function with respect to $\ddot{\boldsymbol{x}}_i$, one may obtain:

$$\begin{aligned} \boldsymbol{S}^* := \frac{\partial S}{\partial\ddot{\boldsymbol{x}}_i} &= m\,\frac{\partial\vec{\boldsymbol{a}}_P}{\partial\ddot{\boldsymbol{x}}}\cdot\vec{\boldsymbol{a}}_P + \frac{\partial\vec{\boldsymbol{\alpha}}}{\partial\ddot{\boldsymbol{x}}}\cdot[\boldsymbol{I}_P\,\vec{\boldsymbol{\alpha}}] + \frac{\partial\vec{\boldsymbol{\alpha}}}{\partial\ddot{\boldsymbol{x}}}\cdot[\vec{\boldsymbol{\omega}}\times(\boldsymbol{I}_P\,\vec{\boldsymbol{\omega}})] \\ &+ m\,\frac{\partial\vec{\boldsymbol{a}}_P}{\partial\ddot{\boldsymbol{x}}}\cdot[\vec{\boldsymbol{\alpha}}\times\vec{\boldsymbol{\rho}}] + m\,\vec{\boldsymbol{a}}_P\cdot\left[\frac{\partial\vec{\boldsymbol{\alpha}}}{\partial\ddot{\boldsymbol{x}}}\times\vec{\boldsymbol{\rho}}\right] \\ &+ m\,\frac{\partial\vec{\boldsymbol{a}}_P}{\partial\ddot{\boldsymbol{x}}}\cdot[\vec{\boldsymbol{\omega}}\times(\vec{\boldsymbol{\omega}}\times\vec{\boldsymbol{\rho}})]\,. \end{aligned} \tag{7}$$

The generalized forces acting on the robot, $\boldsymbol{U}$, can be obtained as follows:

$$\boldsymbol{J}^{-T}\,\boldsymbol{U} = \boldsymbol{S}^*. \tag{8}$$

The linear and angular velocity of the rigid body can be expressed as

$$\boldsymbol{v}_P = \boldsymbol{J}_L\ \dot{\boldsymbol{x}}, \quad \boldsymbol{\omega} = \boldsymbol{J}_A\ \dot{\boldsymbol{x}}, \tag{9}$$

where, $\boldsymbol{J}_L$ and $\boldsymbol{J}_A$ are called translational and angular Jacobian matrix, respectively. To find acceleration equations one may differentiates from (9), which gives

$$\boldsymbol{a}_P = \boldsymbol{J}_L\ddot{\boldsymbol{x}} + \dot{\boldsymbol{J}}_L\dot{\boldsymbol{x}} - \boldsymbol{\sigma}_g, \quad \alpha = \boldsymbol{J}_A\ddot{\boldsymbol{x}} + \dot{\boldsymbol{J}}_A\dot{\boldsymbol{x}}, \tag{10}$$

in which, $\boldsymbol{\sigma}_g$ denotes the gravity acceleration is added to this formulation to accommodate the gravitational forces. Equation (7) can be expressed as

$$\boldsymbol{S}^* = \boldsymbol{H}(\boldsymbol{x})\,\ddot{\boldsymbol{x}} + \boldsymbol{C}(\boldsymbol{x},\dot{\boldsymbol{x}})\,\dot{\boldsymbol{x}} + \boldsymbol{G}(\boldsymbol{x}) = \boldsymbol{J}^{-T}\,\boldsymbol{U}, \tag{11}$$

where, $\boldsymbol{H}$ matrix of dynamic model is obtained as follows

$$\boldsymbol{H} = \frac{\partial\boldsymbol{S}^*}{\partial\ddot{\boldsymbol{x}}}. \tag{12}$$

The coriolis and centrifugal effects is derived using

$$\boldsymbol{C} = \frac{\partial\boldsymbol{S}^*}{\partial\dot{\boldsymbol{x}}}. \tag{13}$$

Having $\boldsymbol{S}^*$, $\boldsymbol{H}$ and $\boldsymbol{C}$ the gravity term is derived by substitution in

$$\boldsymbol{G} = \boldsymbol{S}^* - \boldsymbol{H}\ddot{\boldsymbol{x}} - \boldsymbol{C}\dot{\boldsymbol{x}}. \tag{14}$$

III. Mathematical Model

A. Physical Description of Eye-RHAS

In Fig. 3 a wire model of Eye-RHAS is presented, so as the geometric description of the robot can be discussed clearly.

B. Kinematics

As mentioned in [13], kinematic analysis refers to the robot geometry and motion study, without considering the forces and torques that cause that motion. To analyse the robot kinematics, forward kinematics (FK) and inverse kinematics (IK) has been studied in the following sub-sections.

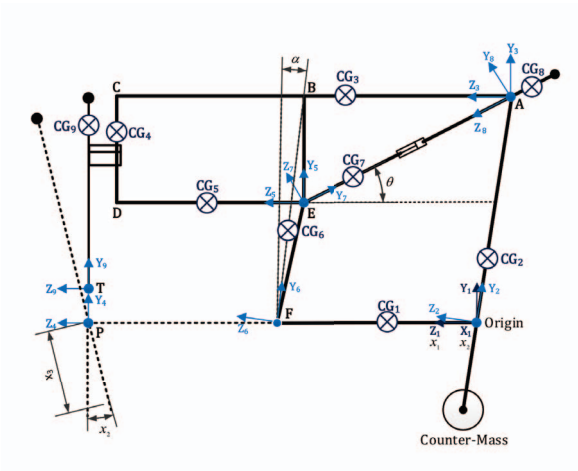

Fig. 3: Wire model of the Eye-RHAS manipulator

1) FK: To show the relation between the task and joint spaces, one may derive FK. According to Fig. 3, this relation for the Eye-RHAS manipulator can be written as follows

$$\begin{aligned} x_T &= -x_3 \cos(x_2) \sin(x_1), \\ y_T &= +x_3 \cos(x_2) \cos(x_1), \\ z_T &= +x_3 \sin(x_2) + L_3. \end{aligned} \tag{15}$$

In Fig.4 the cartesian workspace of this manipulator has been shown.

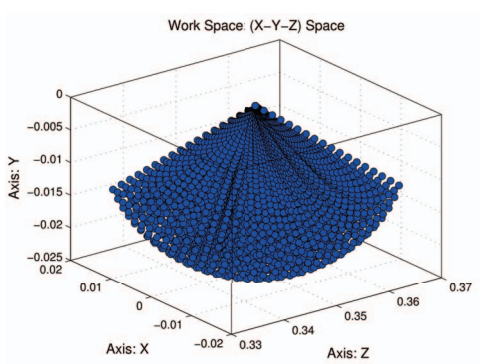

Fig. 4: Manipulator Cartesian Work Space

2) IK: One may have the value of Cartesian variables and wants to calculate the joint variable values. In this situation, IK will be needed. This inverse problem may be solved by the following equation.

$$\begin{aligned} x_3 &= \sqrt{x_T^2 + y_T^2 + z_T^2 - L_3^2}, \\ x_2 &= asin\left(\frac{z_T - L_3}{x_3}\right), \\ x_1 &= atan2\left(-x_T,\, y_T\right). \end{aligned} \tag{16}$$

C. Jacobian Matrix

The analysis of differential kinematics plays a vital role in the study of robotic manipulators. It turns out that the study of velocities in a manipulator leads to the definition of the Jacobian matix. The Jacobian matrix not only reveals the relation between the moving end-effector linear and angular velocities $\dot{\boldsymbol{x}}$ to the actuator joint variables $\dot{\boldsymbol{q}}$, but also constructs the transformation needed to find the actuator forces and moments acting on the end-effector [13]. with Jacobian matrix we have

$$\dot{\boldsymbol{q}} = \boldsymbol{J}\, \dot{\boldsymbol{x}}. \tag{17}$$

Reffering to the kinematics of Eye-RHAS, the task space variables, $\boldsymbol{x}_1$ and $\boldsymbol{x}_3$ are directly actuated via joint variables, $\boldsymbol{q}_1$ and $\boldsymbol{q}_3$, respectively. But the motion of $\boldsymbol{x}_2$ is produced indirectly, using a linear mechanism as shown in Fig.3. Based on the structure of Eye-RHAS, Jacobian matrix can be written as the decoupled form

$$\boldsymbol{J} = \begin{bmatrix} 1 & 0 & 0 \\ 0 & J_{22} & 0 \\ 0 & 0 & 1 \end{bmatrix}, \tag{18}$$

where,

$$J_{22} = -\frac{l_4 \cos(x_2)\, [\, l_3 - l_5 \,]}{\sqrt{l_4^2 \cos^2(x_2) + [\, l_5 - l_3 + l_4 \sin(x_2) \,]^2}}. \tag{19}$$

D. Dynamics

Dynamic analysis is needed for the mechanical design, motion simulation, calibration and control of the robot. In this work, GA approach has been used to derive the dynamic matrices of the robot in the general closed form formulation given in (1). By using (12) - (14), these matrices may be written as follows,

$$\begin{aligned} \boldsymbol{H}(\boldsymbol{x}) &= \begin{bmatrix} H_{11} & 0 & 0 \\ 0 & H_{22} & H_{23} \\ 0 & H_{32} & H_{33} \end{bmatrix}, \\ \boldsymbol{C}(\boldsymbol{x}, \dot{\boldsymbol{x}}) &= \begin{bmatrix} C_{11} & C_{12} & C_{13} \\ C_{21} & C_{22} & C_{23} \\ C_{31} & C_{23} & 0 \end{bmatrix}, \quad \boldsymbol{G}(\boldsymbol{x}) = \begin{bmatrix} G_1 \\ G_2 \\ G_3 \end{bmatrix}. \end{aligned} \tag{20}$$

To avoid clutter, the non-zero elements of H, C, and G has been expressed in appendix.A

IV. Experimental Results

A. Dynamics Verification

In this work SimMechanics Toolbox has been used to verify the calculated closed-form dynamics model derived in (20). For this means, the embodiment of Eye-RHAS, shown in Fig. 5, plays the role of the real robot. The parameter values used in this model are given in tables I and II.

For sake of verification, the following trajectory in task space coordinate is considered for the robot.

$$\boldsymbol{x}(t) = \mathbf{a} \cdot \sin\left[\mathbf{b} + 2\,\pi\left(\mathbf{f}_0\, t + \frac{\mathbf{k}}{2}\, t^2\right)\right], \tag{21}$$

in which, $\mathbf{a} = [0.35,\, 0.1,\, 0.1]^T$, $\mathbf{b} = \mathbf{f_0} = [0,\, 0,\, 0]^T$, and $\mathbf{k} = [0.10,\, 0.09,\, 0.08]^T$ are constant vectors.

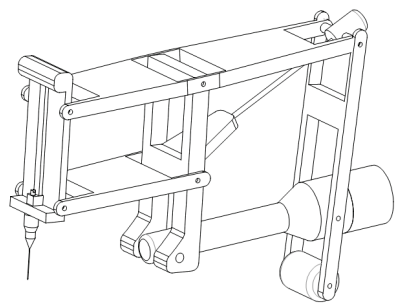

Fig. 5: Eye-RHAS CAD Model

TABLE I: Body Tensors ($I_r = I_{zy}$)

I_x	(g/m^2)	I_y	(g/m^2)	I_z	(g/m^2)	I_r	(g/m^2)
I_{x_1}	1.2	I_{y_1}	1.2	I_{z_1}	0.048	I_{r_1}	0
I_{x_2}	4.32	I_{y_2}	1.08	I_{z_2}	3.41	I_{r_2}	0
I_{x_3}	1.7	I_{y_3}	1.7	I_{z_3}	0.065	I_{r_3}	0
I_{x_4}	1.07	I_{y_4}	0.267	I_{z_4}	0.811	I_{r_4}	0.4
I_{x_5}	0.067	I_{y_5}	0.067	I_{z_5}	0.003	I_{r_5}	0
I_{x_6}	0.635	I_{y_6}	0.135	I_{z_6}	0.522	I_{r_6}	0
I_{x_7}	0.036	I_{y_7}	0.004	I_{z_7}	0.032	I_{r_7}	0
I_{x_8}	0.081	I_{y_8}	0.081	I_{z_8}	0.001	I_{r_8}	0
I_{x_9}	0.325	I_{y_9}	0.037	I_{z_9}	0.294	I_{r_9}	0

TABLE II: Body Properties

Mass	(g)	Length	(cm)	COM	(cm)
m_1	90	l_1	20	(x_1, y_1, z_1)	$(0, 0, 10)$
m_2	400	l_2	18	(x_2, y_2, z_2)	$(0, 9, 0)$
m_3	40	l_3	35	(x_3, y_3, z_3)	$(0, 0, 18)$
m_4	80	l_4	10	(x_4, y_4, z_4)	(0, 10, -5)
m_5	10	l_5	15	(x_5, y_5, z_5)	$(0, 0, 7)$
m_6	50	l_{cm}	7	(x_6, y_6, z_6)	$(0, 10, 0)$
m_7	20			(x_7, y_7, z_7)	$(0, 4, 0)$
m_8	45			(x_8, y_8, z_8)	(0, 0, -4)
m_9	45			(x_9, y_9, z_9)	$(0, 8, 0)$

The results of dynamics verification is shown in Fig. 6. In the top part of this figure, the trajectories in three different axes are shown. The second part of this figure illustrates the dynamic efforts required to generate such trajectories, calculated from the closed form dynamics of the robot. Finally the bottom part of this figure shows the difference between these efforts from the one obtained through SimMechanics simulations. As it is seen in this figure, the results obtained from dynamics formulation, is identical to that obtained from SimMechanics implementation with the precision of 10^{-14}. By this means the formulation is verified with the required accuracy.

B. Trajectory Control

Once the dynamic formulation is verified, it may be used in different applications. In here a trajectory control in a teleoperation application is considered. In order to perform such task, as it is shown in Fig. 7, the simulated robot is used in a real-time teleoperation loop, considering an inverse dynamics control scheme [15], in which the PD control gains are set to $k_p = 30$ and $k_d = 3$, by trial and error. In order to generate the required trajectories in such application, a PHANToM Omni

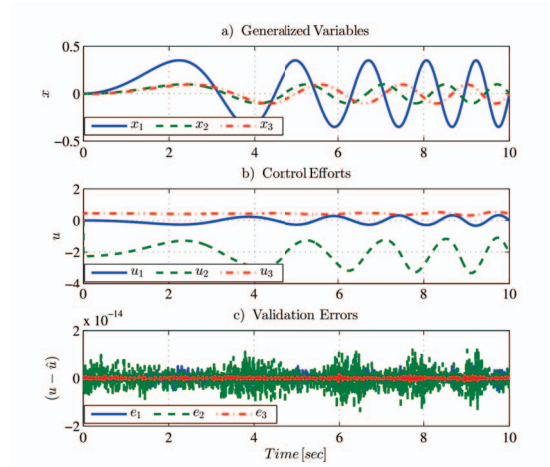

Fig. 6: Validation Results

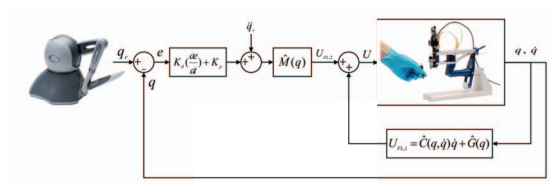

Fig. 7: The general structure of the IDC scheme

haptic device is used within an xpc-target routine in MATLAB for real time simulation. The result of one of such experiments are shown in Fig. 8 and 9. In the first figure an offline step response in three axes is requested for the robot, and as it is seen in this figure, the controller is capable to perform well in practice. The transient response is very well suited, while zero steady state error is obtained. In the second experiment, which is shown in Fig. 9, the trajectories is generated by the operator in a real time experiments, while the robot is tracking the desired trajectories with the required precision. The control efforts required to perform such task is shown in the bottom part of this figure, which are well beyond the available limits. This experiments, provides the required assurance to perform further real time teleoperation tasks in future experiments.

V. Conclusion

In this research a closed-form dynamical model of Eye-RHAS manipulator has been derived by GA method. The verification scheme which has been performed on the virtual model, in SimMechanics Toolbox, shows the precision of the derived dynamics. To evaluate the model, off-line step response and real-time performance has been studied, and the results guarantee that this model may be used for future practical design problems.

VI. Appendix A

The non-zero elements of (20) are as follows, with the inertia elements

$$H_{11} = s_5 \left[I_{r8} c_5 + (I_{y8} + I_{z7}) s_5\right] + I_{z2} {c_4}^2 + (I_{z4} + I_{z9})\, {c_2}^2 + m_8\, l_2\, c_4 \left[2\,(c_5\, y_8 - s_5\, z_8) + l_2\, c_4\right] + (I_{y4} + I_{y9})\, {s_2}^2$$

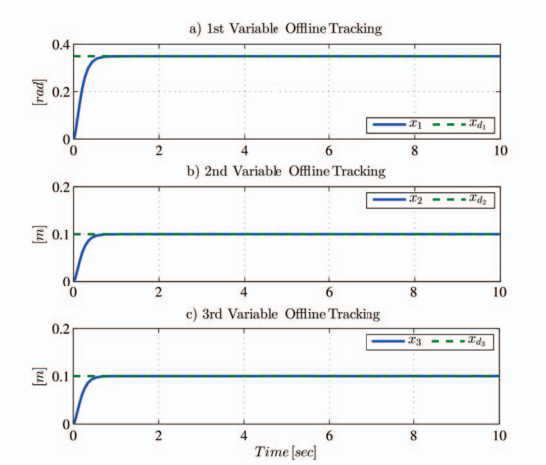

Fig. 8: Off-line step response tracking performance

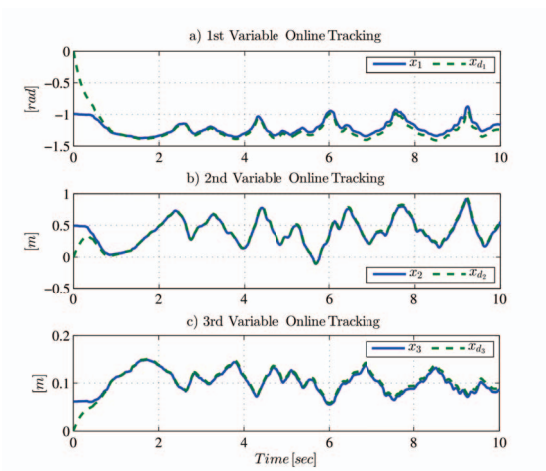

Fig. 9: On-line Evaluation Results

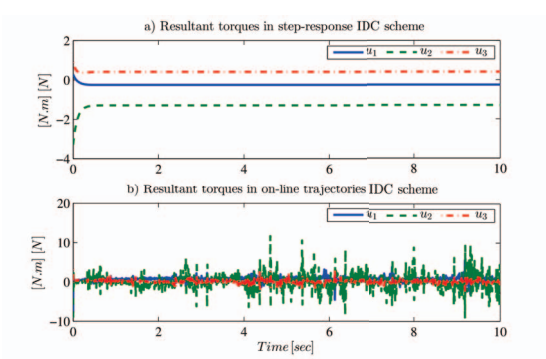

Fig. 10: Resultant control efforts in online and offline modes

$$
\begin{aligned}
&+ m_9\, x_3\, c_2\, [(x_3 + 2\, y_9)\, c_2 - 2\, z_9\, s_2] + (I_{y_2} + I_{y_6})\, {s_4}^2 \\
&+ m_7\, (c_2\, l_4 - c_4\, l_2)\, [c_2\, l_4 - c_4\, l_2 - 2\, (c_5\, z_7 + s_5\, y_7)] \\
&+ m_5\, (c_2\, l_4 - c_4\, l_2)\, (c_2\, l_4 - c_4\, l_2 - 2\, y_5) + I_{z6} {c_4}^2 \\
&+ c_5\, [c_5 (I_{y_7} + I_{z8}) + s_5 (I_{r8} - I_{r7})] - I_{r7}\, c_5\, s_5 \\
&+ I_{z1} + I_{z3} + I_{z5} + m_3\, l_2\, \left(l_2\, {c_4}^2 + 2\, y_3\, c_4\right) \\
&+ 2\, (I_{r4} + I_{r9})\, c_2\, s_2 - 2\, (I_{r2} + I_{r6})\, c_4\, s_4 \qquad (22)
\end{aligned}
$$

$$
\begin{aligned}
H_{22} &= m_3\, l_2^2 + m_9 x_3\, (2y_9 + x_3) + I_{x7}\, F_{12}^2 + \Gamma_7 \\
&\quad + m_5\, \Gamma_6 + m_7\, (\Gamma_4 + \Gamma_5) - 2\, m_8\, l_2\, z_8\, s_6\, F_{12} \qquad (23) \\
H_{33} &= m_9 \qquad (24) \\
H_{23} &= H_{32} = -m_9\, z_9 \qquad (25)
\end{aligned}
$$

The elements of Coriolis and centrifugal matrix, C_{ij}, are given as follows.

$$
\begin{aligned}
C_{11} &= l_2\, s_4\, \dot{x}_2 [m_3 (y_3 + c_4\, l_2) + m_8 (c_4\, l_2 + c_5\, y_8 - s_5\, z_8)] \\
&\quad + m_7\, \dot{x}_2\, (l_2\, s_4 + l_4\, s_2)\, (c_4\, l_2 - c_2\, l_4 + c_5\, z_7 + s_5\, y_7) \\
&\quad + \dot{x}_2\, [c_2\, (I_{r9}\, c_2 - I_{z9}\, s_2) + s_2\, (I_{y9}\, c_2 - I_{r9}\, s_2)] \\
&\quad + \dot{x}_2\, c_5\, [I_{r8}\, c_5 - I_{z8}\, s_5 - (I_{r7}\, c_5 + I_{y7}\, s_5)] F_{12} \\
&\quad + \dot{x}_2\, s_5\, [I_{z7}\, c_5 + I_{r7}\, s_5 + I_{y_8}\, c_5 - I_{r8}\, s_5]\, F_{12} \\
&\quad + m_9\, (c_2\, \dot{x}_3 - \dot{x}_2\, s_2\, x_3)\, (c_2\, x_3 + c_2\, y_9 - s_2\, z_9) \\
&\quad - \dot{x}_2\, [I_{r2}\, (2\, {s_4}^2 - 1) + I_{y_2}\, c_4\, s_4 - I_{z2}\, c_4\, s_4] \\
&\quad - \dot{x}_2\, [I_{r6}\, (2\, {s_4}^2 - 1) + I_{y_6}\, c_4\, s_4 - I_{z6}\, c_4\, s_4] \\
&\quad - \dot{x}_2\, [I_{r4}\, (2\, {s_2}^2 - 1) - I_{y_4}\, c_2\, s_2 + I_{z4}\, c_2\, s_2] \\
&\quad + m_5\, \dot{x}_2\, (l_2\, s_4 + l_4\, s_2)\, (y_5 - c_2\, l_4 + c_4\, l_2) \\
&\quad + m_7\, \dot{x}_2\, (c_2\, l_4 - c_4\, l_2)\, (s_5\, z_7 - c_5\, y_7)\, F_{12} \\
&\quad - m_8\, c_4\, \dot{x}_2\, l_2\, (z_8\, c_5 + y_8\, s_5)\, F_{12} \\
&\quad - m_9\, \dot{x}_2\, x_3\, c_2\, (z_9\, c_2 + y_9\, s_2) \qquad (26) \\
C_{12} &= m_8 l_2 s_4 \dot{x}_1 (c_4 l_2 + c_5 y_8 - s_5 z_8) + \dot{x}_1 c_4 (I_{r2} c_4 - I_{y_2} s_4) \\
&\quad + \dot{x}_1 m_7 (c_4 l_2 - c_2 l_4 + c_5 z_7 + s_5 y_7)(L + l_2 s_4 + l_4 s_2) \\
&\quad - c_5\, \dot{x}_1\, [I_{r7}\, c_5 - I_{z7}\, s_5 + m_7\, y_7\, (c_2\, l_4 - c_4\, l_2)]\, F_{12} \\
&\quad + s_5\, \dot{x}_1\, [I_{r7}\, s_5 - I_{y_7}\, c_5 + m_7\, z_7\, (c_2\, l_4 - c_4\, l_2)]\, F_{12} \\
&\quad + \dot{x}_1\, c_4\, (I_{r6}\, c_4 - I_{y_6}\, s_4) + \dot{x}_1\, l_2\, m_3\, s_4\, (y_3 + c_4\, l_2) \\
&\quad + \dot{x}_1\, s_4\, (I_{z2}\, c_4 - I_{r2}\, s_4) + \dot{x}_1\, s_4\, (I_{z6}\, c_4 - I_{r6}\, s_4) \\
&\quad + \dot{x}_1\, m_5\, (y_5 - c_2\, l_4 + c_4\, l_2)\, (L + l_2\, s_4 + l_4\, s_2) \\
&\quad - \dot{x}_1\, [I_{r4}\, (2\, {s_2}^2 - 1) - I_{y_4}\, c_2\, s_2 + I_{z4}\, c_2\, s_2] \\
&\quad - \dot{x}_1\, s_5\, (I_{z8}\, c_5 + I_{r8}\, s_5 + c_4\, l_2\, m_8\, y_8)\, F_{12} \\
&\quad + \dot{x}_1\, c_5\, (I_{r8}\, c_5 + I_{y_8}\, s_5 - c_4\, l_2\, m_8\, z_8)\, F_{12} \\
&\quad + \dot{x}_1\, c_2\, (I_{r9}\, c_2 + I_{y_9}\, s_2 - c_2\, m_9\, x_3\, z_9) \\
&\quad - \dot{x}_1\, s_2\, (I_{z9}\, c_2 + I_{r9}\, s_2 + c_2\, m_9\, x_3\, y_9) \\
&\quad - m_9\, s_2\, x_3\, \dot{x}_1 (c_2\, x_3 + c_2\, y_9 - s_2\, z_9) \qquad (27) \\
C_{13} &= m_9\, c_2\, \dot{x}_1\, (c_2\, x_3 + c_2\, y_9 - s_2\, z_9) \qquad (28) \\
C_{21} &= m_7\, c_5\, \dot{x}_1\, (c_2\, l_4 - c_4\, l_2)(L c_5 + l_2\, s_6 - l_4\, s_7 + F_{12}\, y_7) \\
&\quad - m_7\, s_5\, \dot{x}_1\, (c_2\, l_4 - c_4\, l_2)(c_6\, l_2 - c_7\, l_4 - L s_5 + F_{12}\, z_7) \\
&\quad - \dot{x}_1\, [c_5\, (I_{r8}\, c_5 - I_{z8}\, s_5) + s_5\, (I_{y_8}\, c_5 - I_{r8}\, s_5)]\, F_{12} \\
&\quad - m_7\, c_5\, (c_5\, \dot{x}_1\, z_7 + \dot{x}_1\, s_5\, y_7)\, (L c_5 + l_2\, s_6 - l_4\, s_7) \\
&\quad - m_7\, s_5\, (c_5\, \dot{x}_1\, z_7 + \dot{x}_1\, s_5\, y_7)\, (c_7\, l_4 - c_6\, l_2 + L s_5) \\
&\quad + [s_5\, (f_1\, y_8 + c_6\, f_2\, l_2) + c_5\, (f_1\, z_8 - f_2\, l_2\, s_6)]\, \Sigma_2 \\
&\quad - \dot{x}_1\, m_5\, (y_5 - c_2\, l_4 + c_4\, l_2)\, (L + l_2\, s_4 + l_4\, s_2) \\
&\quad + \dot{x}_1\, [I_{r4}\, (2\, {s_2}^2 - 1) - I_{y_4}\, c_2\, s_2 + I_{z4}\, c_2\, s_2] \\
&\quad + \dot{x}_1\, [I_{r2}\, (2\, {s_4}^2 - 1) + I_{y_2}\, c_4\, s_4 - I_{z2}\, c_4\, s_4] \\
&\quad + \dot{x}_1\, [I_{r6}\, (2\, {s_4}^2 - 1) + I_{y_6}\, c_4\, s_4 - I_{z6}\, c_4\, s_4] \\
&\quad + m_8\, l_2\, \dot{x}_1 (c_5\, y_8 - s_5\, z_8)(c_6\, s_5 - c_5 s_6)
\end{aligned}
$$

$$
\begin{aligned}
&- m_3\, l_2\, \dot{x}_1\, (s_4\, y_3 + c_4\, l_2\, s_4) + \Sigma_1 \\
&+ c_5\, (I_{r7}\, c_5\, \dot{x}_1 + I_{y7}\, s_5\, \dot{x}_1)\, F_{12} \\
&- s_5\, (I_{z7}\, c_5\, \dot{x}_1 + I_{r7}\, s_5\, \dot{x}_1)\, F_{12} \qquad (29)\\
C_{22} = {} & m_7\, \dot{x}_2\, (l_2\, s_6 - l_4\, s_7)\, (l_2\, c_6 - l_4\, c_7 - L\, s_5 + F_{12}\, z_7) \\
&- m_7\, \dot{x}_2\, (c_6\, l_2 - c_7\, l_4)\, (L\, c_5 + l_2\, s_6 - l_4\, s_7 + F_{12}\, y_7) \\
&- m_7\, z_7\, f_2\, [(c_7\, l_4 - c_6\, l_2 + Ls_5) + I_{x7}\, F_{12}]\, \Sigma_4 \\
&+ (I_{x8}\, f_1 + c_6\, f_2\, l_2\, m_8\, y_8 - f_2\, l_2\, m_8\, s_6\, z_8)\, \Sigma_4 \\
&+ m_5\, L\, \dot{x}_2\, (c_2\, l_4 - c_4\, l_2) + m_9\, \dot{x}_3\, (x_3 + y_9) \\
&- [\dot{x}_2\, m_7\, z_7\, (Lc_5 + l_2\, s_6 - l_4\, s_7)]\; F_{12}^2 \\
&- [\dot{x}_2\, m_7\, y_7\, (Ls_5 + l_4\, c_7 - l_2\, c_6)]\; F_{12}^2 \\
&- m_8\, l_2\, F_{12}^2\, \dot{x}_2\, (c_6\, z_8 + s_6\, y_8) + \Sigma_3 \\
&+ m_7\, y_7\, f_2\, (Lc_5 + l_2\, s_6 - l_4\, s_7)\, \Sigma_4 \qquad (30)\\
C_{23} = {} & m_9\, \dot{x}_2\; (x_3 + y_9) \qquad (31)\\
C_{31} = {} & -m_9\, c_2\, \dot{x}_1\; (c_2\, x_3 + y_9\, c_2 - z_9\, s_2) \qquad (32)\\
C_{32} = {} & -m_9\, \dot{x}_2\; (x_3 + y_9) \qquad (33)\\
C_{33} = {} & 0 \qquad (34)
\end{aligned}
$$

The elements of the gravitational terms, G_i, are given as:

$$
\begin{aligned}
G_1 = {} & [g_x\, c_1 + g_y\, s_1]\, [\, m_1\, y_1 + m_2\, (y_2\, c_4 + z_2\, s_4) \\
&+ m_5\, (y_5 - l_4\, c_2 + l_2\, c_4) + m_6\, (z_6\, s_4 + y_6\, c_4) \\
&+ m_3\, (\, y_3 + l_2\, c_4) + m_4\, (y_4\, c_2 - z_4\, s_2) \\
&+ m_7\, (l_2 c_4 - l_4 c_2 + z_7 c_5 + y_7 s_5) \\
&+ m_8\, (l_2\, c_4 + y_8\, c_5 - z_8\, s_5) \\
&+ m_9\, (x_3\, c_2 - z_9\, s_2 + y_9\, c_2\,)\,] \qquad (35)\\
G_2 = {} & g_z\, m_5\; (l_4\, c_2 - l_2\, c_4) - m_9\, (x_3 + y_9)\, \Lambda_4 \\
&+ m_4\, z_4\; (g_z\, s_2 + g_y\, c_1\, c_2 - g_x\, c_2\, s_1) \\
&- m_2\, z_2\; (g_z\, s_4 - g_y\, c_1\, c_4 + g_x\, c_4\, s_1) \\
&- m_6\, z_6\; (g_z\, s_4 - g_y\, c_1\, c_4 + \; g_x c_4\, s_1) \\
&+ m_9\, z_9\; (g_z\, s_2 + g_y\, c_1\, c_2 - g_x\, c_2\, s_1) \\
&- m_4\, y_4\; (c_2\, g_z - g_y\, c_1\, s_2 + g_x\, s_1\, s_2) \\
&- m_2\, y_2\; (c_4\, g_z + g_y\, c_1\, s_4 - g_x\, s_1\, s_4) \\
&- m_6\, y_6\; (c_4\, g_z + g_y\, c_1\, s_4 - g_x\, s_1\, s_4) \\
&- m_7 \Lambda_1\, (g_z\, s_5 + g_y\, c_1\, c_5 - g_x\, c_5\, s_1) \\
&- m_7 \Lambda_2\, (g_z\, c_5 - g_y\, c_1\, s_5 + g_x\, s_1\, s_5) \\
&- m_8\, (\Lambda_5\, \Lambda_8 + \Lambda_6\, \Lambda_9) - m_3\, l_2\, \Lambda_7 \\
&- m_5 \Lambda_3\, (g_y\, c_1 - g_x\, s_1) \qquad (36)\\
G_3 = {} & -m_9\, (g_z\, s_2 + g_y\, c_1\, c_2 - g_x\, c_2\, s_1) \qquad (37)
\end{aligned}
$$

where the notations are as follows

$$
\begin{aligned}
&c_1 := \cos(x_1)\,, && s_1 := \sin(x_1) \\
&c_2 := \cos(x_2)\,, && s_2 := \sin(x_2) \\
&c_3 := \cos(x_3)\,, && s_3 := \sin(x_3) \\
&c_4 := \cos(\alpha - x_2)\,, && s_4 := \sin(\alpha - x_2) \\
&c_5 := \cos(\theta)\,, && s_5 := \sin(\theta) \\
&c_6 := \cos(\alpha + \theta - x_2)\,, && s_6 := \sin(\alpha + \theta - x_2) \\
&c_7 := \cos(\theta - x_2)\,, && s_7 := \sin(\theta - x_2) \\
&f_1 := l_4\, (l_4 - l_3\, s_2 + l_5\, s_2)\, (l_5 - l_3 + l_4\, s_2)^{-2} \\
&f_2 := 1 + \tan^2(\theta), \quad L := l_1 + l_5 - l_3 \\
&F_{12} := f_1 f_2^{-1}, \quad \theta := -\tan\left(\frac{l_4\, c_2}{l_5 - l_3 + l_4\, s_2}\right) \\
&\Gamma_1 := \left[I_{x8}\, f_1^2 + m_8\, l_2\, f_2\; (l_2\, f_2 + 2\, y_8\, c_6\, f_1)\right] f_2^{-2} \\
&\Gamma_2 := 2\, m_7\, y_7\; (L\, c_5 + l_2\, s_6 - l_4\, s_7)\, F_{12} \\
&\Gamma_3 := 2\, m_7\, z_7\; (L\, s_5 + l_4\, c_7 - l_2\, c_6)\, F_{12} \\
&\Gamma_4 := (L\, c_5 + l_2\, s_6 - l_4\, s_7)^2 \\
&\Gamma_5 := (L\, s_5 + l_4\, c_7 - l_2\, c_6)^2 \\
&\Gamma_6 := (c_2 l_4 - c_4 l_2)^2 + (L + l_2 s_4 + l_4 s_2)^2 \\
&\Gamma_7 := \Gamma_1 + \Gamma_2 - \Gamma_3 + I_{x2} + I_{x4} + I_{x6} + I_{x9} \\
&\Sigma_1 := 0.5\, \dot{x}_1\, [2\, I_{r9}\, (2\, {s_2}^2 - 1) - 2\, I_{y9}\, c_2\, s_2 + 2\, I_{z9}\, c_2\, s_2] \\
&\qquad - 0.5\, \dot{x}_1\, [2\, m_9\, x_3\, z_9\, (2\, {s_2}^2 - 1) - 2\, c_2\, m_9\, s_2\, {x_3}^2] \\
&\Sigma_2 := m_8\, l_2\, c_4\, \dot{x}_1\, f_2^{-1} \\
&\Sigma_3 := m_8\, l_2\, \dot{x}_2\, f_2^{-1} [s_6\, (f_1\, y_8 + c_6\, f_2\, l_2) + c_6\, (f_1\, z_8 - f_2\, l_2\, s_6)] \\
&\qquad + 0.5\, \dot{x}_1\, [4\, c_2\, m_9\, s_2\, x_3\, y_9] \\
&\Sigma_4 := \Sigma_f\, f_2^{-3}, \quad \Sigma_f := \dot{f}_1\, f_2 - \dot{f}_2\, f_1 \\
&\Lambda_1 := +L\, c_5 + l_2\, s_6 - l_4\, s_7 + y_7\, F_{12} \\
&\Lambda_2 := -L\, s_5 + l_2\, c_6 - l_4\, c_7 + z_7\, F_{12} \\
&\Lambda_3 := L + l_2\, s_4 + l_4\, s_2 \\
&\Lambda_4 := g_z\, c_2 - g_y\, c_1\, s_2 + g_x\, s_1\, s_2 \\
&\Lambda_5 := g_z\, c_5 - g_y\, c_1\, s_5 + g_x\, s_1\, s_5 \\
&\Lambda_6 := g_z\, s_5 + g_y\, c_1\, c_5 - g_x\, s_1\, c_5 \\
&\Lambda_7 := g_z\, c_4 + s_4\, (g_y\, c_1 - g_x\, s_1) \\
&\Lambda_8 := l_2\, c_6 + y_8\, F_{12} \\
&\Lambda_9 := l_2\, s_6 - z_8\, F_{12} \qquad (38)
\end{aligned}
$$

REFERENCES

[1] Media centre: Fact Sheet N 282. Visual impairment and blindness, August 2014. [www.who.int, online access: June 01 2014].

[2] H Meenink, R Hendrix, G Naus, M Beelen, H Nijmeijer, M Steinbuch, E Oosterhout, and M Smet. Robot-assisted vitreoretinal surgery. *Ed.), Medical robotics: minimally invasive surgery. Cornwall: Woodhead Publishing Limited*, pages 185–209, 2012.

[3] Mayo Clinic Staff. Tests and procedures: Robotic surgery, 1998-2015. [www.MayoClinic.org, online access: June 01 2014].

[4] Meenink T. *Vitreo-Retinal eye surgery robot: sustainable precision*. PhD thesis, TU Eindhoven, Eindhoven, The Netherlands, ISBN: 978-90-386-2800-4, 2011.

[5] V. Mata, S. Provenzano, F. Valero, and JI. Cuadrado. Serial-robot dynamics algorithms for moderately large numbers of joints. *Mechanism and machine Theory*, 37(8):739–755, 2002.

[6] A. Valera, V. Mata, M. Valles, F. Valero, N. Rosillo, and F. Benimeli. Solving the inverse dynamic control for low cost real-time industrial robot control applications. *Robotica*, 21:261–269, 6 2003.

[7] E. Abedloo, A. Molaei, and H.D. Taghirad. Closed-form dynamic formulation of spherical parallel manipulators by gibbs-appell method. In *Robotics and Mechatronics (ICRoM), 2014 Second RSI/ISM International Conference on*, pages 576–581, Oct 2014.

[8] The mathworks. inc. simmechanics user's guide, March 2007.

[9] 3D Touch Components: Hardware Installation PHANToM Omni and technical Manual. Sensable technologies. *Revision 6.5*, 2000.

[10] Sheridan T. B. Telerobotics. *Automatica*, 25(4):487–507, 1989.

[11] Peter F. Hokayem and Mark W. Spong. Bilateral teleoperation: An historical survey. *Automatica*, 42:2035–2057, 2006.

[12] Jean-Jacques. E. Slotine and Weiping Li. On the adaptive control of robot manipulators. *The International Journal of Robotics Research*, 6(3):49–59, 1987.

[13] Hamid D Taghirad. *Parallel Robots: Mechanics and Control*. CRC Press, 2013.

[14] J. Ginsberg. *Engineering Dynamics*, pages 23–67. Number v. 10 in Engineering dynamics. Cambridge University Press, 2008.

[15] Mark W Spong and Mathukumalli Vidyasagar. *Robot dynamics and control*. John Wiley & Sons, 2008.